

Helical Ribbon Aggregate Composed of a Crown-Appended Cholesterol Derivative Which Acts as an Amphiphilic Gelator of Organic Solvents and as a Template for Chiral Silica Transcription

Jong Hwa Jung,^{†,‡} Hedeki Kobayashi,[†] Mitsutoshi Masuda,[§] Toshimi Shimizu,[§] and Seiji Shinkai^{†,*}

Contribution from the Chemotransfiguration Project, Japan Science and Technology Corporation (JST), 2432 Aikawa, Kurume, Fukuoka 839-0861, Japan, and Nanoarchitectonics Research Center, National Institute of Advanced Industrial Science and Technology (AIST), Tsukuba Central 5, 1-1-1 Higashi, Tsukuba, Ibaraki 305-8565, Japan

Received February 26, 2001

Abstract: New crown-appended cholesterol-based organogelator **1**, which has two cholesterol skeletons as a chiral aggregate-forming site, two amino groups as an acidic proton-binding site, and one crown moiety as a cation-binding site, was synthesized, and the gelation ability was evaluated in organic solvents. It can gelate acetic acid, acetonitrile, acetone, ethanol, 1-butanol, 1-hexanol, DMSO, and DMF under 1.0 wt %, indicating that **1** acts as a versatile gelator of various organic solvents. To characterize the aggregation mode in the organogel system, we observed a CD spectrum of the acetic acid gel **1**. In the CD spectrum, the $\lambda_{\theta=0}$ value appears at 353 nm, which is the same as the absorption maximum $\lambda_{\text{max}} = 353$ nm. The positive sign for the first Cotton effect indicates that the dipole moments of azobenzene chromophores tend to orient in a clockwise direction. Very surprisingly, the TEM images of the **1** + acetic acid gel resulted in the helical ribbon and the tubular structures. Sol–gel polymerization of tetraethoxysilane was carried out using **1** in the gel phase. The silica obtained from the **1** + acetic acid gel showed the helical ribbon with 1700–1800-nm pitches and the tubular structure of the silica with ~ 560 -nm outer diameter. As far as can be recognized, all the helicity possesses a right-handed helical motif. Since the exciton-coupling band of the organogel also shows *R* (right-handed) helicity, we consider that a microscopic helicity is reflected by a macroscopic helicity.

Introduction

The sol–gel synthesis of well-ordered inorganic materials offers a new and wide-ranging approach to useful materials with controlled architecture and porosity across a range of length scales.^{1,2} The direct synthesis of discrete inorganic architectures necessitates the use of dispersed organic supramolecular structures with commensurate dimensionality; for example, hollow fibers of silica have been prepared with self-assembled viroid cylinders,¹ organic crystals,^{2c} or phospholipid fibers^{2f} as templates.

Recently, numerous thermoreversible physical gels formed with low-molecular-weight organic molecules have been reported.^{3–7} The interest shown lies in the numerous potential applications envisaged for these materials such as hardeners of solvents, drug delivery systems, membranes, and sensors. Very recently, organogels were applied as novel media to produce

various structures of silica such as linear fibers,^{8a,b} lamellar,^{8c–e} helical fibers,^{8f} and spherical^{8g} structures by sol–gel polymerization. These results indicate that the superstructures formed in organogels are useful as templates to create various silica structures. One particularly interesting class of gelators, crown-appended cholesterol-based gelators, frequently resulted in

* Corresponding author: (fax) +81-942-39-9012; (e-mail) seijitcm@mbox.nc.kyushu-u.ac.jp.

[†] Japan Science and Technology Corp.

[‡] Present address: CREST, JST, Nanoarchitectonics Research Center, National Institute of Advanced Industrial Science and Technology (AIST), Tsukuba Central 4, 1-1-1 Higashi, Tsukuba, Ibaraki 305-8562, Japan.

[§] National Institute of Advanced Industrial Science and Technology.

(1) Mann, S., Ed. *Biomimetic Materials Chemistry*; VCH: New York, 1996.

(2) (a) Shenton, W.; Douglas, T.; Young, M.; Stubbs, G.; Mann, S. *Adv. Mater.* **1999**, *11*, 253. (b) Douglas, T.; Young, M. *Nature* **1998**, *393*, 152. (c) Shenton, W.; Pum, D.; Sleytr, U.; Mann, S. *Nature* **1997**, *389*, 585. (d) Davis, S. A.; Burkett, S. L.; Mendelson, N. H.; Mann, S. *Nature* **1997**, *385*, 420. (e) Nakamura, H.; Matsui, Y. *J. Am. Chem. Soc.* **1995**, *117*, 2651. (f) Burkett, S. L.; Mann, S. *Chem. Commun.* **1996**, 321. (g) Shenton, W.; Douglas, T.; Young, M.; Stubbs, G.; Mann, S. *Adv. Mater.* **1999**, *11*, 253.

(3) (a) Murata, K.; Aoki, M.; Suzuki, T.; Harada, T.; Kawabata, H.; Komori, T.; Ohseto, F.; Ueda, K.; Shinkai, S. *J. Am. Chem. Soc.* **1994**, *116*, 6664 and references therein. (b) James, T. D.; Murata, K.; Harada, T.; Ueda, K.; Shinkai, S. *Chem. Lett.* **1994**, 273. (c) Jeong, S. W.; Murata, K.; Shinkai, S. *Supramol. Sci.* **1996**, *3*, 83. (d) Shinkai, S.; Murata, K. *J. Mater. Chem.* **1998**, *8*, 485. (e) Yoza, K.; Amanokura, N.; Ono, Y.; Akao, T.; Shinmori, H.; Takeuchi, M.; Shinkai, S.; Reinhout, D. L. *Chem. Eur. J.* **1999**, *5*, 2722.

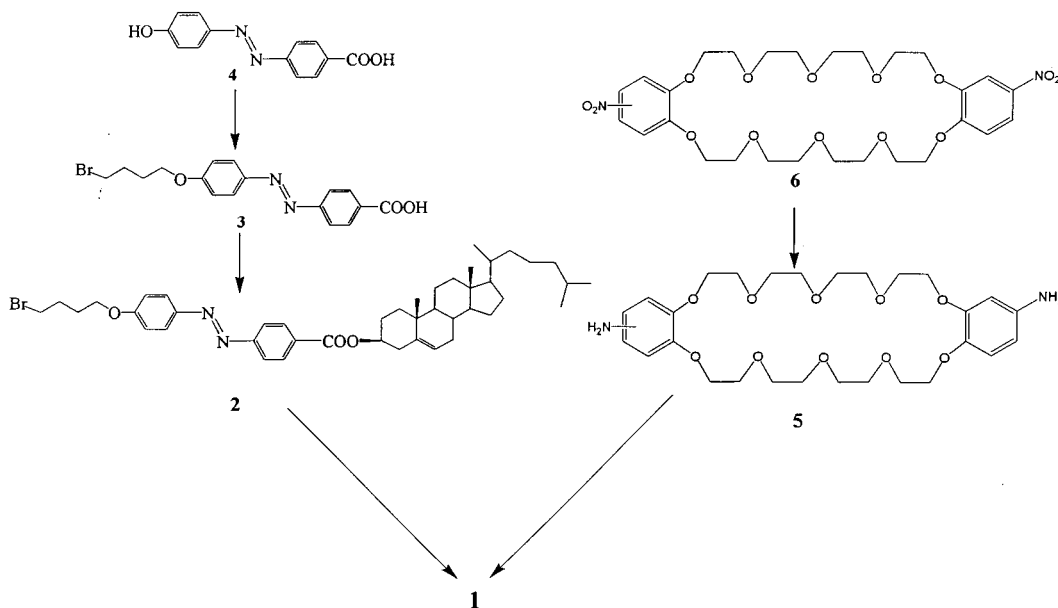
(4) (a) Wang, R.; Geiger, C.; Chen, L.; Swanson, B.; Whitten, D. G. *J. Am. Chem. Soc.* **2000**, *122*, 2399. (b) Duncan, D. C.; Whitten, D. G. *Langmuir* **2000**, *16*, 6445. (c) Geiger, C.; Stanescu, M.; Chen, L.; Whitten, D. G. *Langmuir* **1999**, *15*, 2241.

(5) (a) For recent comprehensive reviews, see: Terech, P.; Weiss, R. G. *Chem. Rev.* **1997**, 3313. (b) Otsuni, E.; Kamaras, P.; Weiss, R. G. *Angew. Chem., Int. Ed. Engl.* **1996**, *35*, 1324 and references therein. (c) Terech, P.; Furman, I.; Weiss, R. G. *J. Phys. Chem.* **1995**, *99*, 9558 and references therein.

(6) (a) Hanabusa, K.; Yamada, M.; Kimura, M.; Shirai, H. *Angew. Chem., Int. Ed. Engl.* **1996**, *35*, 1949. (b) Loos, M.; Esch, J. v.; Stokroos, I.; Kellogg, R. M.; Feringa, B. L. *J. Am. Chem. Soc.* **1997**, *119*, 12675. (c) Schoonbeek, F. S.; Esch, J. v.; Hulst, R.; Kellogg, R. M.; Feringa, B. L. *Chem. Eur. J.* **2000**, *6*, 2633. (d) Esch, J. v.; Feringa, B. L. *Angew. Chem., Int. Ed.* **2000**, *39*, 2263.

(7) (a) Melendez, R.; Geib, S. J.; Hamilton, A. D. In *Molecular Self-Assembly Versus Inorganic Approaches*; Fujita, M., Ed.; Springer: Berlin, **2000**. (b) Carr, A. J.; Melendez, R.; Geib, S. J.; Hamilton, A. D. *Tetrahedron Lett.* **1998**, *39*, 7447. (c) Shi, C.; Kilic, S.; Xu, J.; Enick, R. M.; Beckman, E. J.; Carr, A. J.; Melendez, R. E.; Hamilton, A. D. *Science* **1999**, *286*, 1540.

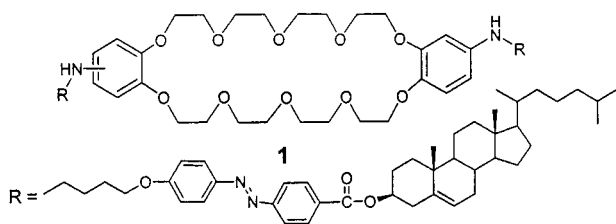
Scheme 1



various novel structures such as the fibrous, the lamellar,^{8d} the vesicular,^{8g} and the multilayered tubular^{8c} structures.

Kunitake and co-workers found that certain amphiphiles can form the tubular structure through the helical ribbon structure in aqueous solution.⁹ They possess a polar head and suitable chiral hydrophobic groups to form stable aggregates. Also, the formation of twisted ribbon structures of gelators were reported by a number of research groups.^{5,10} However, they were not grown from the helical ribbon or the tubular structures through a twisted ribbon structure. Helical ribbon structures of the organogels, on the other hand, were never observed in organic solvent systems, and it thus occurred to us that judging from the versatility of crown-appended cholesterol-based gelators,^{8e,d,g} one might be able to find both structures, growing from the helical ribbon to the tubule (as suggested by Kunitake et al.⁹ for the aqueous solution system). In addition, superstructures created from these gelators might be useful as templates for transcription into the silica structures.

With these objects in mind, we have designed **1**, which has



two cholesterol skeletons as a chiral aggregate-forming site, two amino groups as an acidic proton-binding site, and one crown moiety as a cation-binding site. We have found that **1** not only

(8) (a) Ono, Y.; Nakashima, K.; Sano, M.; Kanekiyo, Y.; Inoue, K.; Hojo, J.; Shinkai, S. *Chem. Commun.* **1998**, 1477. (b) Ono, Y.; Kanekiyo, Y.; Inoue, K.; Hojo, J.; Shinkai, S. *Chem. Lett.* **1999**, 23. (c) Jung, J. H.; Ono, Y.; Shinkai, S. *Langmuir* **2000**, *16*, 1643. (d) Jung, J. H.; Ono, Y.; Shinkai, S.; *J. Chem. Soc., Perkin Trans. 2* **1999**, 1289. (e) Jung, J. H.; Ono, Y.; Shinkai, S. *Angew. Chem., Int. Ed.* **2000**, *39*, 1862. (f) Jung, J. H.; Ono, Y.; Shinkai, S. *Chem. Eur. J.* **2000**, *5*, 4552. (g) Jung, J. H.; Ono, Y.; Sakurai, K.; Sano, M.; Shinkai, S. *J. Am. Chem. Soc.* **2000**, *122*, 8648.

(9) (a) Nakashima, N.; Asakuma, S.; Kunitake, T. *J. Am. Chem. Soc.* **1985**, *107*, 09. (b) Fuhrhop, J.-H.; Köning, J. *Membranes and Molecular Assemblies: The Synergistic Approach*; Royal Society of Chemistry: London, 1994; and references therein. (c) Kunitake, T. *Angew. Chem., Int. Ed. Engl.* **1992**, *21*, 709. (d) Nakashima, N.; Kunitake, T. *Chem. Lett.* **1984**, 1709.

Table 1. Gelation Ability of **1** in Organic Solvents^a

entry	solvent	gelation ^b
1	acetic acid	G
2	propionic acid	G
3	acetonitrile	G
4	acetone	G
5	ethanol	G
6	1-butanol	G
7	1-hexanol	G
8	DMSO	G
9	DMF	G
10	chloroform	S
11	tetrahydrofurane	S
12	<i>n</i> -hexane	I

^a Gelator concentration, 1.0 wt %. ^b Gelation of **1**: G, stable gel formed at room temperature; S, soluble; I, insoluble.

gelates various organic solvents under 1.0 wt % but enables us to observe both the helical ribbon and the tubule. In addition, it acts as a template for sol-gel polymerization of tetraethoxysilane (TEOS) to produce the novel "helical ribbon silica" as well as the "double-layered tubular silica". To the best of our knowledge, this is the first observation not only for the helical ribbon structure in the organogel system but also for the direct transcription of the molecular assemblies into the helical ribbon structure of the silica.

Results and Discussion

Characterization of Organogel Superstructure by Circular Dichroism (CD). Compound **1** was synthesized according to Scheme 1. The gelation ability of **1** was estimated in various organic solvents. The results are summarized in Table 1. The gelator **1** could gelate 8 out of 12 organic solvents under 1.0 wt %, indicating that **1** acts as a versatile gelator of various organic solvents. Gelator **1** formed better gel in organic solvents in comparison to gelators bearing small size crown moiety such as 24-crown-8- and 18-crown-6-appended gelators.

To characterize the aggregation mode in the organogel phase, we observed the CD spectrum of acetic acid gel **1**. In the CD spectrum, the $\lambda_{\theta=0}$ value appears at 353 nm, which is consistent

(10) (a) Oda, R.; Huc, I.; Candau, S. J. *Angew. Chem., Int. Ed.* **1998**, *37*, 2689. (b) Menger, F. M.; Keiper, J. S. *Angew. Chem., Int. Ed.* **2000**, *41*, 1906.

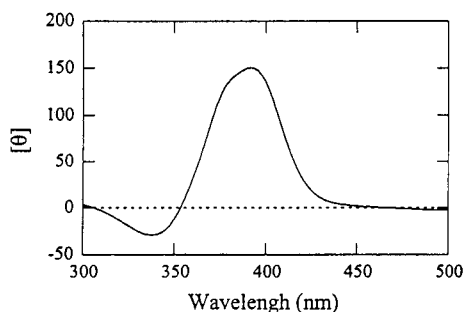


Figure 1. CD spectrum of the **1** + acetic acid gel.



Figure 2. TEM picture of the xerogel **1** prepared from acetic acid (negatively stained with UO_2^{2+}).

with the absorption maximum at $\lambda_{\text{max}} = 353$ nm. One can thus assign the CD spectrum to the exciton-coupling band, although it is somewhat asymmetrical (Figure 1). It is known that azobenzene-appended cholesterol gelators with natural (*S*) C-3 configuration tend to give a positive sign for the first Cotton effect, indicating that the dipole moments of azobenzene chromophores tend to orient in a clockwise direction.^{8e,f} However, the macroscopic helicity of the aggregate formed by self-assembly is not necessarily related to the microscopic helicity in a Cotton effect. This problem will be discussed later in more detail. We confirmed that the contribution of linear dichroism (LD) to the true CD spectrum is negligible by using the conventional LD mode. The strong CD intensity suggests, therefore, that **1** in the organogel adopts a folded conformation to enjoy efficient intramolecular cholesterol–cholesterol and azobenzene–azobenzene interactions.¹¹

Helical and Tubular Structures of the Organogel As Observed by Transmission Electron Microscopy (TEM). To obtain visual insights into the aggregation mode, we observed the xerogel structure of acetic acid gel **1** by TEM and scanning electron microscopy (SEM). Figure 2 shows a TEM picture of the xerogel **1** obtained from acetic acid. Very interestingly, the xerogel **1** mainly consists of the tubular structures with ~ 520 -nm outer diameter but also illustrates the linear ribbon and the helical ribbon with 1700–1800-nm pitch. The organogel **1** possesses a right-handed helical motif, since the exciton-coupling band of the organogel **1** also shows *R* helicity. In addition, the SEM picture of the xerogel **1** also reveals the characteristic right-handed helical ribbon structure. These results indicate that the structure of the organogel process involves several metastable intermediate structures, viz. the linear ribbon \rightarrow the helical ribbon \rightarrow the tubule. The structure of **1** is quite different from double-chain ammonium amphiphiles previously reported by Kunitake et al. which have long aliphatic groups.⁹ These amphiphiles were transformed from the helical ribbon structure (its presence is assumed) into the tubular structure with ~ 3.2 - μm diameter in aqueous solution by sonication, whereas **1** can form both the helical ribbon structure and the tubular structure with ~ 520 -nm diameter and 1700–1800-nm pitch,

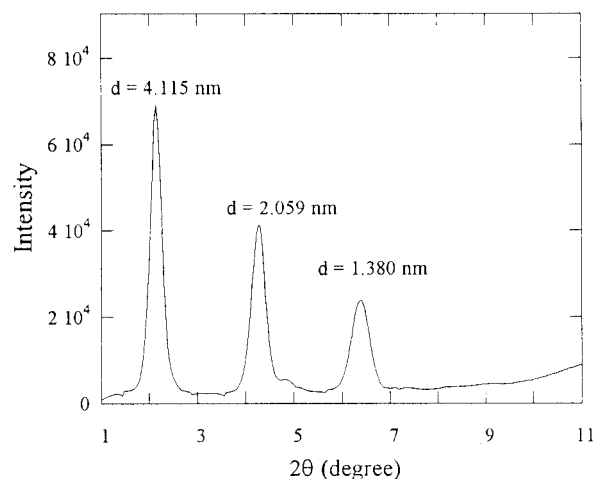


Figure 3. Powder XRD spectrum of xerogel **1** prepared from acetic acid.

respectively, even in organic solvents without sonication. The organogel morphology is clearly different between azacrown-appended gelator and **1**; azacrown-appended gelator gave the vesicular structure^{8g} whereas **1** gave the helical ribbon structure. This implies that the helical ribbon structure in the organogel **1** grows more efficiently from the vesicular structure than that in the azacrown-appended gelator. It is not clear yet, however, why the further growth of the vesicular structure is suppressed in azacrown-appended gelator whereas it continues to grow to the “helical ribbon structure” in **1**.

Recently, an X-ray crystallographic methodology for ascertaining the molecular packing of gelators in the gel phase has been reported, and this method is being used to clarify the gelation mechanism of low-molecular-weight gelators.¹² However, the correlation between the molecular packing of gelator molecules and the physical gelation properties is still unknown. The xerogel **1** obtained from acetic acid by a freezing method resulted in the spongelike aggregate but not the typical crystal. We obtained information about the molecular-packing mode of gelator molecules in a neat gel from an X-ray diffraction pattern of the xerogel. The diffraction pattern is characterized by three sharp reflection peaks of 41.15, 20.59, and 13.80 Å (Figure 3), the relative intensity of which is almost exactly in the ratio of $1:1/2:1/3$. This means that the xerogel maintains a layered structure with the interlayer distance of 41.15 Å corresponding to the (100) plane, while that of sample **1** prepared by conventional synthetic procedures gave only a broad pattern. This result supports the view that the organogel possesses the well-ordered aggregate structure in the gel state.

Sol–Gel Polymerization of TEOS and SEM/TEM Observation of the Silica Structure. To transcribe the superstructure formed in the organogel into the silica structure, we carried out sol–gel polymerization of TEOS using **1** in acetic acid or 1-butanol gel phase according to the method described previously.⁸ After sol–gel polymerization, we observed SEM pictures of the silica obtained from **1** before and after calcination. Figure 4 shows a SEM picture after calcination: the silica obtained from acetic acid **1** possesses the helical ribbon structure with 1700–1800-nm pitches and the tubular structure of the silica

(11) A similar folded conformation was proposed for an azacrown derivative bearing two cholesterol groups.^{8g}

(12) (a) Hanabusa, K.; Matsumoto, M.; Kimura, M.; Kakehi, A.; Shirai, H. *J. Colloid Interface Sci.* **2000**, *224*, 231. (b) Abdallah, D. J.; Sirchio, S.; Weiss, R. G. *Langmuir* **2000**, *16*, 7558. (c) Sakurai, K.; Ono, Y.; Jung, J. H.; Okamoto, S.; Sakurai, S.; Shinkai, S. *J. Chem. Soc., Perkin Trans. 2* **2001**, 108.



Figure 4. SEM picture of the silica obtained from the **1** + acetic acid gel after calcination.

with ~560-nm outer diameter. As far as can be recognized, all the helicity possesses a right-handed helical motif. Since the exciton-coupling band of the organogel also shows *R* (right) helicity, we consider that in the present system a microscopic helicity is reflected by a macroscopic helicity. These results indicate that the novel helical ribbon structure and the tubular structure of the organogel **1** have successfully been transcribed into the silica structures. This helical ribbon silica structure is novel and different from the helical fiber structures obtained from cyclohexanediamine-based organogels.^{8f}

To further corroborate that the organogel structure really acted as a template for growth of the helical ribbon into the tubule, TEM pictures were taken after removal of **1** by calcination (Figure 5). Very interestingly, 1700–1800 nm of the helical pitches of the helical ribbon structure remains constant with a gradual change into the tubular structure (FigureS 5a–c). In addition, the silica illustrates double layers with an interlayer distance of 8–9 nm (Figure 5d). These results indicate that TEOS (or oligomeric silica particles) was adsorbed onto both surfaces of the double-layered tubules with 8–9-nm thickness. Therefore, the tubular silica possesses two hollow cavities. The smaller hollow with 8–9-nm layers was created by the organogel template whereas the larger hollow with 460–480-nm inner diameters was created by the growth of helical ribbon. We believe that such a precise transcription becomes possible for the first time by using the organogel superstructures as a template featuring the crystal-like characters. In addition, sol–gel polymerization of TEOS using a large crown-appended gelator such as **1** in the presence of metal salts and organic compounds can be conveniently applied to deposition of noble metals and organic compounds in the 8–9-nm interlayers of the helical ribbon structure of the silica. In contrast, the deposition of noble metals on the inner wall in the helical fiber of the silica prepared from the cyclohexanediamine gels is very difficult or almost impossible.

The helical ribbon and the tubular structures of the silica were also created in 1-butanol where the amino groups are not protonated. The result again supports the importance of the intermolecular hydrogen-bonding interaction in the creation of the helical ribbon and the tubular structures (Figure 6a). When a trace amount of acid is present in the sol–gel medium, the amino groups are protonated and the cationic charges thus formed can be a driving force to adsorb anionic oligomeric silica particles. To obtain evidence for the contribution of the hydrogen-bonding interaction to the binding of oligomeric silica particles, sol–gel polymerization was carried out in the presence of Et₄NOH (tetraethylammonium hydroxide: 2 equiv to **1**). As expected, the silica produced under this condition also shows the helical ribbon and the tubular structures. This result indicates that the hydrogen-bonding interaction between TEOS and the neutral amino groups of **1** can also act as a driving force to create the novel structure of the silica (Figure 6b).

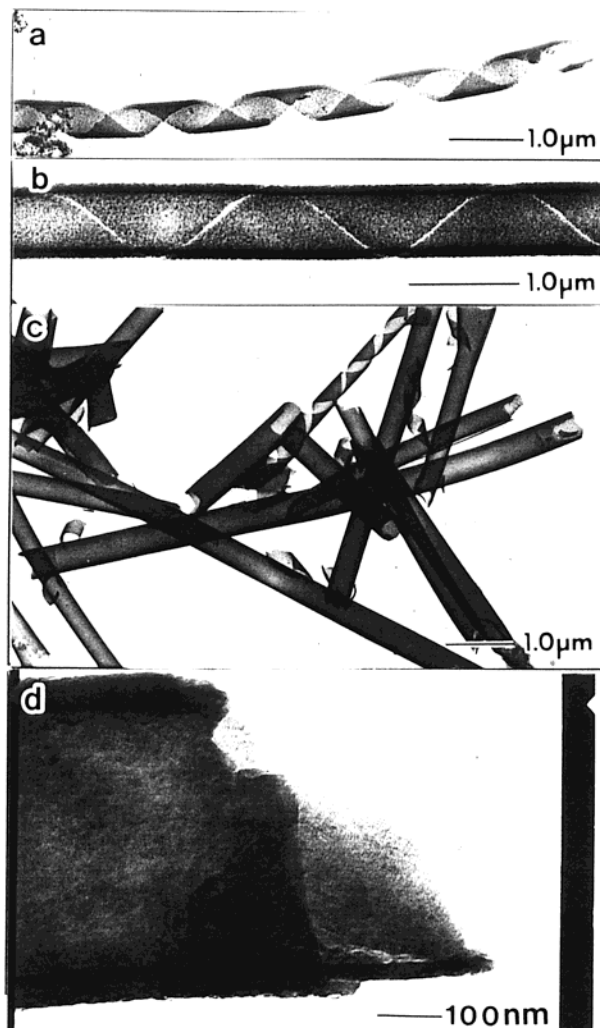


Figure 5. TEM pictures of the silica obtained from the **1** + acetic acid gel after calcination.

Conclusions

The present paper has demonstrated that the organogelator **1** bearing dibenzo-30-crown-10 creates the novel helical and tubular structures in organic solvent. Sol–gel polymerization of TEOS in the presence of the helical structure of **1** is useful to create the helical ribbon structure of the silica. This is a very rare example of chiral inorganic materials. The helical ribbon structures of the silica are created with aid of hydrogen-bonding as well as electrostatic interactions. The results clearly indicate the versatility of the template method in the gel phase for the creation of various silica structures.

In addition, noble metals and organic compounds can be not only conveniently deposited between the layers of the helical ribbon structure of the silica obtained from the organogel **1** by the host–guest interaction¹³ but also readily applicable to the design of novel solid catalysts featuring a size recognition ability of 8–9-nm silica layers. We believe that the present silica with the helical higher-order morphology is useful as unique catalysts for asymmetric syntheses without chiral organic ligands.¹⁴

(13) The feasibility of this idea (deposition of noble metals during the sol–gel process) has been examined; see: References 8d,g, Jung, J. H.; Shinkai, S. *J. Chem. Soc., Perkin Trans. 2* **2000**, 2393.

(14) To test this intriguing idea, we applied this helical silica to the Soai reaction (see: Soai, K.; Osanai, S.; Kadowaki, K.; Yonekubo, S.; Shibata, T.; Sato, I. *J. Am. Chem. Soc.* **1999**, *121*, 11235) in collaboration with Soai's group. Surprisingly, optical yields of 96–98% ee have been attained.

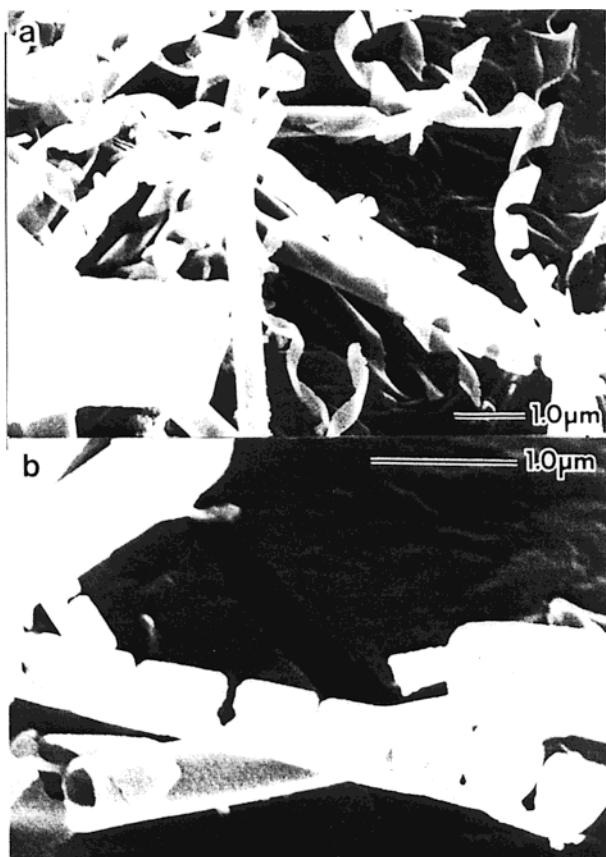


Figure 6. SEM pictures of the silica obtained from the **1** + 1-butanol gel in (a) the absence and (b) the presence of tetraethylammonium hydroxide.

Experimental Section

Apparatus for Spectroscopy Measurements. ^1H and ^{13}C NMR spectra were measured on a Bruker ARX 300 apparatus. IR spectra were obtained in KBr pellets using a Shimadzu FT-IR 8100 spectrometer, and MS spectra were obtained by a Hitachi M-250 mass spectrometer.

TEM and SEM Observations. For TEM, a piece of the gel was placed on a carbon-coating copper grid (400 mesh) and removed after 1 min, leaving some small patches of the gel on the grid. After the specimen was dried at low pressure, it was stained with 10–15- μL drops of uranyl acetate (2.0 wt % aqueous solution). Then, this was dried for 1 h at low pressure. The specimen was examined with a Hitachi H-7100 SEM, using an accelerating voltage of 75–100 kv and a 16-nm working distance. SEM was taken on a Hitachi S-4500. The silica was coated with palladium–platinum and observed at 5–15 kV of the accelerating voltage and an emission current of 10 μA .

Gelation Test of Organic Fluids. The gelator and the solvent were put in a septum-capped test tube and heated in an oil bath until the solid was dissolved. The solution was cooled at room temperature. If the stable gel was observed at this stage, it was classified as G in Table 1.

Sol–Gel Polymerization of TEOS. In a typical preparation, $(1.0\text{--}2.5) \times 10^{-3}$ M gelator was dissolved in acetic acid or 1-butanol. The organogel sample was added to TEOS (15.0–20.0 mg)/water (2.0–6.0 mg) or TEOS (15.0–20.0 mg)/water (2.0–6.0 mg)/benzylamine (2.0–6.0 mg) as a catalyst and warmed until a transparent solution was obtained. Then, the reaction mixture was placed at room temperature under static conditions for 7–14 days. The product was dried by a vacuum pump at room temperature. Finally, the gelator was removed by calcination at 200 $^{\circ}\text{C}$ for 2 h, 500 $^{\circ}\text{C}$ for 2 h under a nitrogen atmosphere, and 500 $^{\circ}\text{C}$ for 4 h under aerobic conditions.

4-(Hydroxyphenyl)azobenzoic Acid (4) and **4-(*n*-Monobromobutoxy-phenyl)azobenzoic acid (3).** These compounds were prepared as described previously.^{8a,c}

4-*n*-Monobromobutoxy-4'-((cholesteryloxy)carbonyl)azobenzene (2). 4-((Bromobutoxyphenyl)azo)benzoic acid **3** (0.7 g, 1.86 mmol) and cholesterol (0.718 g, 2.23 mmol) were dissolved in 20 mL of dichloromethane under a nitrogen atmosphere. The solution was maintained at 0 $^{\circ}\text{C}$ by an ice bath. Dicyclohexylcarbodiimide (DCC; 0.383 g, 1.86 mmol) and (dimethylamino)pyridine (DMAP; 0.022 g, 0.186 mmol) were then added, the reaction mixture being stirred for 4 h at 0 $^{\circ}\text{C}$. The reaction mixture was filtered, and the filtrate was washed with acidic and basic aqueous solutions (50 mL each). The organic layer was evaporated to dryness. The residue was purified by a silica gel column eluting with THF/*n*-hexane (1:6 v/v) to give **2** in 26% yield as a yellow solid (mp 141.5 $^{\circ}\text{C}$). ^1H NMR (300 MHz, CDCl_3): δ (ppm) 8.17 (2H, d, $J = 9.0$ Hz), 7.72 (2H, d, $J = 9.0$ Hz), 7.90 (2H, d, $J = 9.0$ Hz), 7.10 (2H, d, $J = 9.0$ Hz), 5.45 (1H, d, $J = 6.3$ Hz), 5.02–4.88 (1H, m), 4.1 (2H, t, $J = 6.3$ Hz), 3.52 (2H, t, $J = 6.2$ Hz), 2.49 (2H, d, $J = 6.2$ Hz), 2.28–0.94 (35H, m), 0.88 (3H, s). ^{13}C NMR (75 MHz, CDCl_3): δ (ppm) 165.1, 161.88, 155.20, 146.98, 139.9, 130.2, 125.18, 122.84, 122.28, 114.72, 67.22, 66.67, 56.67, 56.11, 50.01, 42.30, 39.71, 39.50, 38.20, 37.01, 36.64, 36.17, 35.79, 33.32, 31.92, 31.86, 29.3, 28.32, 28.01, 27.88, 27.78, 24.28, 23.82, 22.83, 22.56, 21.04, 19.38, 19.38, 18.71, 11.86. MS (SIMS): 745 [$\text{M} + \text{H}$] $^+$. IR (KBr): 3005, 1722, 1603, 1579, 1500, 1468, 1284, 1116, 1047 cm^{-1} .

Dinitro-dibenzo-30-crown-10 (6). To a stirred solution of dibenzo-30-crown-10 (0.15 g, 0.28 mmol) in acetic acid (5 mL) and water (1 mL) at 5.0 $^{\circ}\text{C}$ was added dropwise 60% HNO_3 (1 mL). The reaction mixture was warmed to room temperature over period of 30 min and stirred for an additional 2 h at room temperature. Then, 1.0 M NaOH_{aq} was added to the reaction mixture until the solution became neutral. The precipitate was filtered off, to give **5** in 85.0% yield as a yellow powder (mp 133–135 $^{\circ}\text{C}$). ^1H NMR (300 MHz, CDCl_3): δ (ppm) 3.69 (8H, br s), 3.77 (8H, br s), 3.93 (8H, br s), 4.22 (8H, br s), 6.87 (2H, d, $J = 8.4$ Hz), 7.73 (2H, s), 7.84 (2H, d, $J = 8.4$ Hz). IR (KBr): 3005, 2987, 1508, 1210 cm^{-1} ; MS (SIMS): 644.5 [$\text{M} + 2\text{H}$] $^+$. Anal. Calcd for $\text{C}_{29}\text{H}_{42}\text{N}_2\text{O}_{14}$: C, 54.20; H, 6.59; N, 4.36. Found: C, 54.50; H, 6.55; N, 4.30.

Diaminodibenzo-30-crown-10 (5). Dinitrodibenzo-30-crown-10 (0.134 g, 0.21 mmol) was added to dimethylacetamide anhydride (20 mL), and the solution was stirred until the solid was dissolved. Then, 10% Pd–C (0.10 g) was added to the solution, and hydrogen gas was introduced into the solution for 3 h at room temperature. The reaction mixture was filtered to remove Pd–C, and the filtrate was evaporated in vacuo to dryness. The residue was purified by a silica gel column chromatography eluting with methanol/chloroform (1:9 v/v) to give **5** as a brown solid (0.10 g, 84% yield; mp 68–71 $^{\circ}\text{C}$). ^1H NMR (300 MHz, CDCl_3): δ (ppm) 3.48 (4H, br s), 3.68 (8H, br s), 3.74 (8H, br s), 3.84 (8H, br d, $J = 12.4$ Hz), 4.08 (8H, br s), 6.21 (2H, dd, $J = 8.4$, 2.5 Hz), 6.29 (2H, br s), 6.88 (2H, d, $J = 8.4$ Hz). IR (KBr): 3350, 3007, 2985, 1521, 1504, 1340, 1205 cm^{-1} . MS (SIMS): 557.2 [$\text{M} + 2\text{H}$] $^+$. Anal. Calcd for $\text{C}_{29}\text{H}_{42}\text{N}_2\text{O}_{10}$: C, 59.78; H, 7.96; N, 4.81. Found: C, 60.02; H, 7.90; N, 4.53.

4-(Bis(diaminodibenzo-30-crown-10-butoxy)-4'-((cholesteryloxy)carbonyl)azobenzene (1). A mixture of **2** (0.24 g, 0.32 mmol), **5** (0.085 g, 0.15 mmol), and sodium carbonate (0.317 g, 3.00 mmol) in dry butylnitrile (30 mL) was refluxed for 72 h. The solution was filtered after cooling, and the filtrate was evaporated in vacuo to dryness. The residue was purified by an aluminum oxide column chromatography eluting with ethanol/chloroform (1:30 v/v) to give the desired product as a yellow solid (56 mg, 20% yield; mp 168.2–168.7 $^{\circ}\text{C}$). ^1H NMR (300 MHz, CDCl_3): δ (ppm) 0.70 (6H, s), 0.87 (12H, d, $J = 6.6$ Hz), 0.92–2.06 (70H, m), 2.48 (4H, d, $J = 6.4$ Hz), 3.16 (4H, t, $J = 6.4$ Hz), 3.43 (2H, br s), 3.51–3.79 (16H, m), 3.83–3.92 (8H, m), 4.08 (8H, br s), 4.78–4.93 (2H, m), 5.44 (2H, d, $J = 3.9$ Hz), 6.17 (4H, dd, $J = 18.0$, 8.4, 2.4 Hz), 6.22 (2H, br s), 6.27 (2H, d, $J = 2.4$ Hz), 6.75 (4H, dd, $J = 15.4$, 9.1), 7.01 (4H, d, $J = 8.4$ Hz), 7.90 (4H, d, $J = 8.4$ Hz), 7.94 (4H, d, $J = 8.7$ Hz), 8.17 (4H, d, $J = 8.4$ Hz). IR (KBr): 3350, 3007, 2987, 1600, 1585, 1500, 1220 cm^{-1} . MS (SIMS): 1898.6 [$\text{M} + 2\text{H}$] $^+$. Anal. Calcd for $\text{C}_{116}\text{H}_{162}\text{N}_6\text{O}_{16}$: C, 73.46; H, 8.61; N, 4.43. Found: C, 72.71; H, 8.73; N, 4.45.